UCERF3 Finite Earthquake Rupture Surface Catalog

Jeanne L. Hardebeck, US Geological Survey, Menlo Park, CA

Kevin Milner, University of Southern California, Los Angeles, CA

DRAFT – April 3, 2012

1. Summary

Finite rupture surface models were compiled for large (M≥5.9) earthquakes in the UCERF3 catalog, based on published data. This catalog contains the rupture plane location, spatial extent, and orientation, and does not contain any slip information. The finite rupture surface models consist of one or more planes for each earthquake, with each plane represented by a grid of points with 1 km spacing.

The catalog includes finite rupture models for 68 earthquakes (Table 1, Figure 1). The catalog is fairly complete at high magnitudes, with only 12 unmodeled M≥6.5 earthquakes (Table 2), and only 10 unmodeled M≥6.0 earthquakes in the instrumental period since 1932 (Table 3). As can be seen in Tables 2 and 3, the majority of the unmodeled earthquakes are at early times and on the peripheries of the California region: western Nevada, northern Mexico, and the Mendocino area.

2. Finite Rupture Model Sources

The catalog of finite rupture models is based primarily on prior compilations.

2.1. NGA Project Compilation

A set of finite rupture models was previously assembled as part of the "Next Generation of Ground-Motion Attenuation Models" (NGA) project (*Power et al.,* 2008). These models were compiled from published data by *Chiou et al*. (2008). We obtained the NGA source models from P. Spudich (personal communication, June-August, 2011.) All NGA source models for M≥5.9 events within the California area polygon are used.

2.2. Mendocino Area – Rollins and Stein Compilation

Rollins and Stein (2010) compiled finite source models for earthquakes M≥5.9 near- and off-shore of northwestern California, from the region of the Mendocino triple junction to offshore the California-Oregon border. All source models of *Rollins and Stein* (2010) for events within the California area polygon are used, except for earthquakes already present in the NGA database. The source models were obtained in Coulomb format from the authors (C. Rollins, personal communication, August-September, 2011.)

2.3. Historic Earthquakes – Wang, Jackson, and Kagan Compilation

Wang et al. (2009) compiled finite source models for a number of large historic and instrumental earthquakes in California. All finite source models of *Wang et al.* (2009) are used, except for earthquakes already present in the NGA database or in the *Rollins and Stein* (2010) Mendocino compilation. Therefore, we primarily use the *Wang et al.* (2009) compilation for historic earthquakes, with a few exceptions for instrumental events that do not appear in the other compilations. We obtained the finite source models from the authors' web site (http://jumpy.igpp.ucla.edu/~kagan/cal_extended.dat, last accessed January, 2012.)

The *Wang et al.* (2009) compilation represents the finite sources as a set of focal mechanisms at points along the rupture, which we needed to translate into a set of planes. We did this by interpolating between the given focal mechanism locations (lat(i),lon(i)), and assuming that all planes extend from 0 to 12 km depth. For vertical planes, the corners of the *i*th plane are simply:

(lat(i),lon(i),0 km),

(lat(i),lon(i),12 km),

(lat(i+1),lon(i+1),0 km),

(lat(i+1),lon(i+1),12 km).

For dipping planes, where the strike is the azimuth between points *i* and *i*+1, the corners are:

(lat(i)+(6 km*sin(strike)*tan(90-dip)),lon(i)-(6 km*cos(strike)*tan(90-dip)),0 km),

(lat(i)-(6 km*sin(strike)*tan(90-dip)),lon(i)+(6 km*cos(strike)*tan(90-dip)),12 km),

(lat(i+1)+(6 km*sin(strike)*tan(90-dip)),lon(i+1)-(6 km*cos(strike)*tan(90-dip)),0 km),

(lat(i+1)-(6 km*sin(strike)*tan(90-dip)),lon(i+1)+(6 km*cos(strike)*tan(90-dip)),12 km).

2.4. Miscellaneous Other Finite Sources

Other finite source models were taken from the literature. All of these models consist of a single rupture plane, or were approximated by a single plane. In the majority of cases, while the strike, dip, length, and width of the rupture plane were given in the relevant literature, the latitude/longitude coordinates of the corners of the plane were not. In these cases, the corners were read from the relevant figures, or inferred from their positions relative to the earthquake hypocenter. Finite source models were found in the literature for the 1892 M6.6 Vacaville/Winters (*O'Connell et al*., 2001), 1899 M6.7 San Jacinto (*Sanders*, 1993; *Wyss et al*., 2000), 1933 M6.4 Long Beach (*Hauksson and Gross*, 1991), 1937 M6.0 Anza-Borrego (*Sanders et al.*, 1986; *Doser*, 1990a), 1946 M6.3 Walker Pass (*Bawden et al*., 1999), 1947 M6.5 Manix (*Doser*, 1990b), 1954 M6.4 Anza-Borrego (*Sanders et al.*, 1986; *Doser*, 1990a), 1985 M6.1 Kettleman Hills (*Ekstrom et al*., 1992), and 1993 M6.1 Eureka Valley (*Peltzer and Rosen*, 1995) earthquakes.

2.5. Finite Sources Inferred from Focal Mechanisms

For other earthquakes, no finite source model was found in the literature, but a focal mechanism was found. For these events, the strike and dip of the preferred nodal plane was used to define the orientation of the rupture plane, which is centered on the hypocenter. The width of the rupture plane is found assuming that the rupture goes from 0 to 12 km depth, and the length is set to produce the earthquake's known magnitude assuming a 3 MPa stress drop. Most focal mechanisms are taken from the compilation of *Deng and Sykes* (1997), with two additional mechanisms for the 1952 M6.0 Bryson earthquake (*Dehlinger and Bolt*, 1987) and a 1959 M6.1 Dixie Valley aftershock (*Doser*, 1986, 1987) coming from other sources.

3. Finite Rupture Model Implementation

The finite rupture surfaces consist of one or more planes for each earthquake, with each plane represented by a grid of points with 1 km spacing. The top row of grid points are aligned with the top of the plane, and similarly one column of grid points is aligned with one edge of the plane. If there are grid points for the same earthquake that are less than 0.5 km from each other, in places where multiple planes of that earthquake meet, grid points are removed to ensure that all grid spacing for that earthquake is ≥0.5 km.

4. References:

Bawden, G.W., Michael, A.J., Kellogg, L.H. (1999). Birth of a fault: Connecting the Kern County and Walker Pass, California, earthquakes, Geology, 27 (7), pp. 601-604.

Chiou, B., Darragh, R., Gregor, N., Silva, W. (2008). NGA Project Strong-Motion Database, Earthquake Spectra 24, pp. 23-44.

Dehlinger, P., Bolt, B. A. (1987). Earthquakes and Associated Tectonics in a Part of Coastal Central California, Bulletin of the Seismological Society of America, Vol. 77, No. 6, pp. 2056-2073.

Deng, J., Sykes L.R. (1997). Evolution of the stress field in southern California and triggering of moderate-size earthquakes: A 200-year perspective, Journal of Geophysical Research B: Solid Earth, 102 (B5), pp. 9859-9886.

Doser, D.I. (1986). Earthquake Processes in the Rainbow Mountain-Fairview Peak-Dixie Valley, Nevada, Region 1954-1959, Journal of Geophysical Research B: Solid Earth, 91, (B12), pp. 12,572-12,586.

Doser, D.I. (1987). Modeling the Pnl waveforms of the Fairview Peak-Dixie Valley, Nevada, U.S.A. earthquake sequence (1954-1959), Physics of the Earth and Planetary Interiors, 48 (1-2), pp. 64-72.

Doser, D.I. (1990a). Source characteristics of earthquakes along the southern San Jacinto and Imperial fault zones (1937 to 1954), Bulletin Seismological Society of America, 80 (5), pp. 1099-1117.

Doser, D.I. (1990b). A reexamination of the 1947 Manix, California, earthquake sequence and comparison to other sequences within the Mojave block, Bulletin - Seismological Society of America, 80 (2), pp. 267-277.

Ekstrom, G., Stein, R.S., Eaton, J.P., Eberhart-Phillips, D. (1992). Seismicity and geometry of a 110-km-long blind thrust fault: 1. The 1985 Kettleman Hills, California, earthquake, Journal of Geophysical Research, 97 (B4), pp. 4843-4864.

Hauksson, E., Gross, S. (1991). Source parameters of the 1933 Long Beach earthquake, Bulletin - Seismological Society of America, 81 (1), pp. 81-98.

O'Connell, D.R.H., Unruh, J.R., Block, L.V. (2001). Source characterization and ground-motion modeling of the 1892 vacaville-winters earthquake sequence, California, Bulletin of the Seismological Society of America, 91 (6), pp. 1471-1497.

Peltzer, G., Rosen, P. (1995). Surface displacement of the 17 May 1993 Eureka Valley, California, earthquake observed by SAR interferometry, Science, 268 (5215), pp. 1333-1336.

Power. M., Chiou, B., Abrahamson, N., Bozorgnia, Y., Shantz, T., Roblee, C. (2008). An Overview of the NGA Project, Earthquake Spectra 24, pp. 3-21.

Rollins, J.C., Stein, R.S. (2010). Coulomb stress interactions among M ≥ 5.9 earthquakes in the Gorda deformation zone and on the Mendocino Fault Zone, Cascadia subduction zone, and northern San Andreas Fault, Journal of Geophysical Research B: Solid Earth, 115 (12), B12306, doi:10.1029/2009JB007117.

Sanders, C., Magistrale, H., Kanamori, H. (1986). Rupture Patterns and Preshocks of Large Earthquakes in the Southern San Jacinto Fault Zone, Bulletin of the Seismological Society of America, 76 (5), pp. 1187-1206.

Sanders, C.O. (1993). Interaction of the San Jacinto and San Andreas Fault Zones, Southern California: Triggered Earthquake Migration and Coupled Recurrence Intervals, Science, 260, 973-976.

Wang, Q., Jackson, D.D., Kagan, Y. Y. (2009). California Earthquakes, 1800–2007:A Unified Catalog with Moment Magnitudes, Uncertainties, and Focal Mechanisms, Seismological Research Letters 80 (3), 446-457.

Wyss, M., Schorlemmer, D., Wiemer, S. (2000). Mapping asperities by minima of local recurrence time: San Jacinto-Elsinore fault zones, Journal of Geophysical Research B: Solid Earth, 105 (B4), pp. 7829-7844.

event ID	name	year	M	source
---	San Bernardino	1812	7.5	Wang et al. (2009)
---	Ventura	1812	7.1	Wang et al. (2009)
---	Bay Area	1838	7.4	Wang et al. (2009)
---	Volcano Lake, MX	1852	6.5	Deng & Sykes (1997)
---	Fort Tejon	1857	7.9	Wang et al. (2009)
---	Hayward	1868	7.0	Wang et al. (2009)
---	Owens Valley	1872	7.6	Wang et al. (2009)
---	Owens Valley aftershock	1872	6.8	Wang et al. (2009)
---	Owens Valley aftershock	1872	6.8	Deng & Sykes (1997)
---	Diablo Range	1885	6.5	Deng & Sykes (1997)
---	San Jacinto	1890	6.8	Wang et al. (2009)
---	Imperial Vally	1892	7.3	Wang et al. (2009)
---	Vacaville/Winters	1892	6.6	O'Connell et al. (2001)
---	Anza Borrego	1892	6.5	Deng & Sykes (1997)
---	San Jacinto	1899	6.7	Sanders (1993); Wyss et al. (2000)
---	San Francisco	1906	7.8	Wang et al. (2009)
---	Volcano Lake, MX	1915	6.6	Deng & Sykes (1997)
---	San Jacinto	1918	6.8	Wang et al. (2009)
---	Santa Barbara	1925	6.8	Deng & Sykes (1997)
---	Lompoc	1927	7.1	Wang et al. (2009)
3359741	Long Beach	1933	6.4	Hauksson & Gross (1991)
3362656	Guadalupe Victoria	1934	6.4	Wang et al. (2009)
3364162	Anza Borrego	1937	6.0	Sanders et al. (1986); Doser (1990a)
3365279	Imperial Valley	1940	6.9	NGA
3366099	Borrego Mtn	1942	6.6	Wang et al. (2009)
3360174	Walker Pass	1946	6.3	Bawden et al. (1999)
3358945	Manix	1947	6.5	Doser (1990b)
9860350	Desert Hot Springs	1948	6.0	Wang et al. (2009)
3319401	Kern County	1952	7.5	NGA
---	Bryson	1952	6.0	Dehlinger & Bolt (1987)
3299653	Anza Borrego	1954	6.4	Sanders et al. (1986); Doser (1990a)
---	Eureka	1954	6.5	Wang et al. (2009)
---	Dixie Valley aftershock	1959	6.1	Doser (1986,1987)
---	Parkfield	1966	6.0	NGA
3329122	Borrego Mtn	1968	6.6	NGA
3347678	San Fernando	1971	6.6	NGA
3352060	Imperial Valley	1979	6.5	NGA
1053043	Mammoth Lakes	1980	6.1	NGA
1053045	Mammoth Lakes	1980	6.0	NGA
9730174	Victoria, Mexico	1980	6.3	NGA
1056775	off Eureka	1980	6.9	Rollins & Stein (2010)

Table 1: source of finite rupture models

event ID	name	year	M	source
514869	Westmorland	1981	5.9	NGA
1091100	Coalinga	1983	6.7	NGA
17204	Morgan Hill	1984	6.2	NGA
27615	Mendocino Fault Zone	1984	6.6	Rollins & Stein (2010)
52348	Kettleman Hills	1985	6.1	Ekstrom et al. (1992)
700917	N. Palm Springs	1986	6.0	NGA
10085763	Chalfant Valley	1986	6.2	NGA
10083966	off Cape Mendocino	1987	6.0	Rollins & Stein (2010)
731691	Whittier Narrows	1987	5.9	NGA
134894	Elmore Ranch	1987	6.0	NGA
628016	Superstition Hills	1987	6.5	NGA
216859	Loma Prieta	1989	6.9	NGA
228027	Honeydew	1991	6.1	Rollins & Stein (2010)
3019681	Joshua Tree	1992	6.2	NGA
269151	Cape Mendocino	1992	7.2	NGA
268031	off Cape Mendocino	1992	6.5	Rollins & Stein (2010)
268078	off Cape Mendocino	1992	6.6	Rollins & Stein (2010)
3031111	Landers	1992	7.3	NGA
3031425	Big Bear	1992	6.5	Wang et al. (2009)
---	Eureka Valley	1993	6.1	Peltzer & Rosen (1995)
3144585	Northridge	1994	6.7	NGA
9108652	Hector Mine	1999	7.1	NGA
21086915	Mendocino Fault Zone	2000	5.9	Rollins & Stein (2010)
21323712	San Simeon	2003	6.6	NGA
30228270	Parkfield	2004	6.0	NGA
71338066	off Ferndale	2010	6.5	Rollins & Stein (2010)
14607652	El Mayor Cucapah	2010	7.2	NGA

Table 1: source of finite rupture models, *continued*

event ID	location	year	M
---	San Juan Bautista	1840	6.5
---	Reno area, Western NV	1852	7.3
---	Reno area, Pyramid Lake	1860	6.5
---	Santa Cruz Mountains	1865	6.5
---	CA-OR border	1873	6.9
---	Mendecino	1878	7.0
---	Carson Valley	1887	6.5
---	Mendocino	1894	6.5
---	Mendocino County	1898	6.7
---	Mendocino	1918	6.5
---	Humbolt County	1923	7.2
---	Mendocino	1954	6.5

Table 2: M≥6.5 events without finite rupture model

event ID	location	year	M
---	Eureka	1932	6.4
---	Wabuska EQ, NV	1933	6.1
---	Excelsior Mtns, NV	1934	6.3
3362651	Guadalupe Victoria, MX	1934	6.3
---	Tom's Place	1941	6.0
---	Tom's Place	1941	6.0
---	Mendocino	1941	6.4
---	Verdi EQ, Reno, NV	1948	6.0
---	Mendocino	1954	6.5
32322	Point Arena	1984	6.1

Table 3: M≥6 since 1932 without finite rupture model

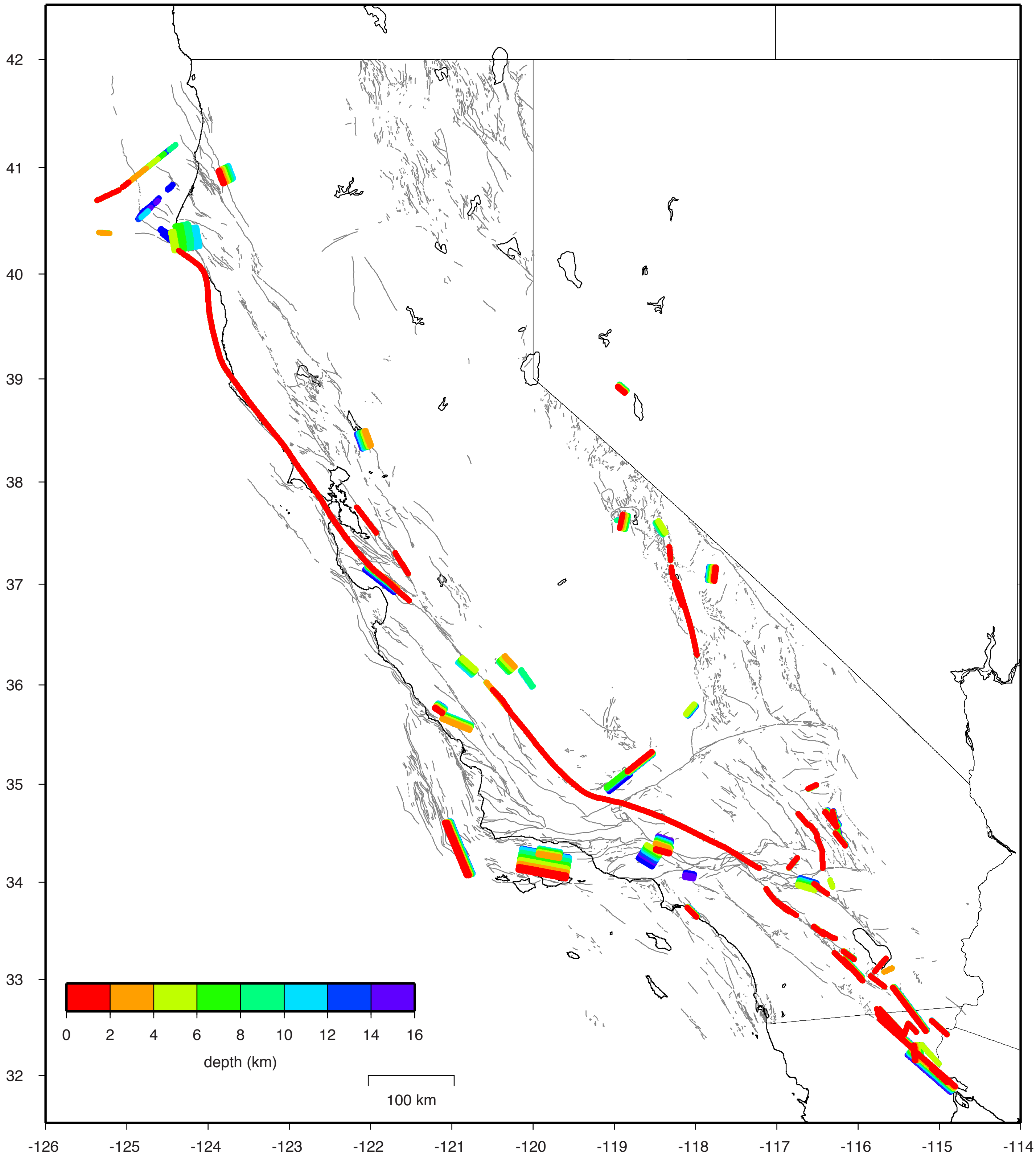

Figure 1. Finite rupture models for 68 California region M≥5.9 earthquakes. Rupture planes are represented and plotted as grids of points with 1 km spacing. Points are plotted in depth order, with shallow points obscuring deeper points for vertical or near-vertical rupture planes.